VOLTAGE STABILITY ASSESMENT BASED ON
TRANSIENT ENERGY FUNCTION

تقدير اتزان الجهد على اساس دالة الطاقة العابرة

A. A. Attia   E. E. Abd-Raboh   H. A. Abd El-Salam
Department of Electrical Power and Machines
Faculty of Engineering
Mansoura University   Tanta University

ملخص: يقترح البحث طريقة لتحليل اتزان الجهد كظاهرة ديناميكية على اساس دالة الطاقة العابرة. ويستخدم فرق الطاقة بين نقط الاتزان و نقط عدم الاتزان التى تناظرها لنفس الحمل لقياس التقارب من انهيار الجهد. ان مشكلة تحديد مجموعة للنقط غير المتزنه لا يمكن حلها ببرنامج سريان القدرة التقليدى نظرا لعدم تقارب الحل عند نقطة انهيار الجهد. و يستخدم البحث برنامج سريان القدرة المستمره لايجاد مجموعة النقط غير المتزنه.

البحث يقدم نتائج تطبيق الطريقة المقترحة على نظامين كهربين. أحدهما نظام نيوانجلاند ١٠ مولدات، ٣٠ قضيب للتحقق من البرنامج ومقارنة النتائج والآخر شبكة مصر الموحدة ممثلة بعدد ٢٤ مولد، ١٠٧ قضبان وقد اخذت حالة التشغيل فى ١٩٩٨/٤/١ كأساس لتحليل النتائج.

ABSTRACT: This paper presents a method to analyze the voltage stability as a dynamic phenomenon based on Transient Energy Function (TEF). The energy difference at equilibrium points is used to measure the proximity to voltage collapse. Problem to identify the set of unstable equilibrium points is solved through the Continuation Power Flow (CPF). Results are demonstrated in detail on the New England 10-machine 30-bus test system and the Egyptian Unified Power Network (EUPN), which is represented by 24-machine 107-bus.

1. INTRODUCTION

Modern electrical power systems are highly interconnected and heavily loaded. As a result, voltage stability and voltage collapse attract more and more attention. A voltage collapse can take place in systems or subsystems and can appear quite abruptly. Continuous monitoring of the system state is therefore required.

There are both static and dynamic aspects involved in voltage stability [1]. But it has been, and still is, analyzed by static approaches. This has resulted from the absence of widely accepted models for the generations and loads, which play the major role in the dynamics of voltage stability [2].

Different methods are established to assess the proximity to voltage collapse. These methods are of two categories. The first determines a static bifurcation then uses it to determine some margin to voltage collapse. The second category calculates some index that has a definite value at the point of collapse [2,3].

In [4], the authors applied energy function method to introduce an energy-based measure of proximity to collapse. This method requires determination of the low voltage power flow solutions (corresponding to the unstable equilibrium points) with lowest associated energy measures. It is a major problem because of Jacobian singularity at the critical point.

In [5], the authors applied a Continuation Power Flow (CPF) technique to obtain this critical point corresponding to voltage instability. The CPF technique using augmented Jacobian avoids the singularity of the Jacobian and in a single run obtains the continuation of power flow solution until the critical point is reached. In this paper, the CPF technique is used to obtain the voltage profile, especially around the critical point, and to identify the set of unstable equilibrium points.

The paper is organized as follows: section 2 discusses the application of energy function method to the problem of voltage stability. In section 3, the basic steps involved in continuation power flow are briefly explained. Section 4 presents algorithm summary. In section 5, the detailed results of studying the New England 10-machine 30-bus test system and the 24-machine 107-bus Egyptian Unified Power Network are demonstrated.

2.   VOLTAGE   STABILITY   ANALYSIS,   USING   TRANSIENT ENERGY FUNCTION

The transient energy function is a technique based on Lyapunov stability theory and originally developed for direct stability analysis of power systems [6,7,8,9]. It is used as a voltage stability index for collapse studies [4]. System transient energy function for n-bus system is [8].

$$TEF = \frac{1}{2}\sum_{k=1}^{n}\sum_{j=1}^{n} B_{kj}\ V_k^o\ V_j^o\ \cos(\delta_k^o - \delta_j^o)$$

$$-\frac{1}{2}\sum_{k=1}^{n}\sum_{j=1}^{n} B_{kj}\ V_k^1\ V_j^1\ \cos(\delta_k^1 - \delta_j^1)$$

$$-\sum_{k=1}^{n} P_k(\lambda_o)(\delta_k^1 - \delta_k^o) - \sum_{k=1}^{n}\int_{V_k^o}^{V_k^1}\frac{Q_k(v,\lambda_o)}{v}dv$$

$$+\sum_{k=1}^{n}\sum_{j=1}^{n} G_{kj}\ V_k^o\ V_j^o\ \cos(\delta_k^o - \delta_j^o)(\delta_k^1 - \delta_k^o)$$

$$+\sum_{k=1}^{n}\sum_{j=1}^{n} G_{kj}\ V_j^o\ \sin(\delta_k^o - \delta_j^o)(V_k^1 - V_k^o)$$

(1)

where

$Y_{kj} = G_{kj} + jB_{kj}$ = transfer admittance between buses k and j

$P_k(\lambda), Q_k(V_k,\lambda)$ = the active and reactive power injections into bus k

$V_k^o \angle \delta_k^o , V_j^o \angle \delta_j^o$ = the phasor bus voltages at s.e.p. (x^o, λ_o)

$V_k^1 \angle \delta_k^1 , V_j^1 \angle \delta_j^1$ = the phasor bus voltages at u.e.p. (x^1, λ_o)

The λ variable represents a scalar parameter or loading factor used to simulate the system load changes that drive the system to collapse. The TEF definition in eqn. (1) provides a measure of the "energy distance" between two equilibrium points. As the system approaches collapse (critical point), $x^o = x^1$ at λ_o and value of the TEF is going to zero. A difficulty with this measure is the computation of the second equilibrium point x^1, particularly for lightly loaded systems.

3. CONTINUATION POWER FLOW

Continuation Power Flow (CPF) is based on locally parameterized continuation technique to avoid the singularity of the Jacobian [5]. Figure 1 shows the steps of the CPF technique, which can summarized as follows:
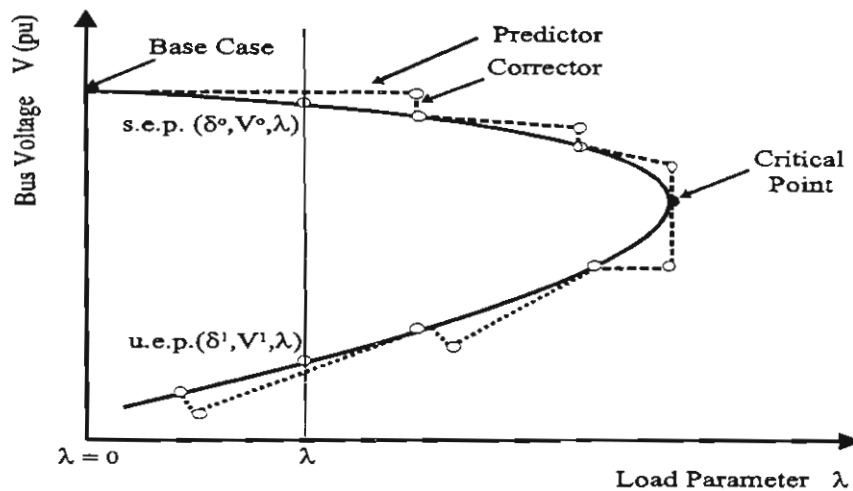
Figure (1): Steps of the CPF method

3.1 Formulation of Power Flow Equations

In order to apply a locally parameterized continuation technique to the power flow problem, a load parameter (λ) must be inserted into equations as follows

$$P_{G\,i}(\lambda) - P_{L\,i}(\lambda) - P_{T\,i} = 0$$
$$Q_{G\,i}(\lambda) - Q_{L\,i}(\lambda) - Q_{T\,i} = 0 \tag{2}$$

where

$$P_{Ti} = \sum_{j=1}^{n} V_i V_j Y_{ij} \cos(\delta_i - \delta_j - \gamma_{ij})$$

$$Q_{Ti} = \sum_{j=1}^{n} V_i V_j Y_{ij} \sin(\delta_i - \delta_j - \gamma_{ij})$$

and $0 \le \lambda \le \lambda_{critical}$. $\lambda = 0$ corresponds to the base case, and $\lambda = \lambda_{critical}$ to the critical case. The subscripts L, G, and T denote bus load, generation, and injection, respectively.

Load Simulation

To simulate a load change, the P_L and Q_{Li} terms can be modified as

$$P_{Li}(\lambda) = P_{Lio} + \lambda(K_{Li}S_{\Delta base} \cos \Psi_i)$$
$$Q_{Li}(\lambda) = Q_{Lio} + \lambda(K_{Li}S_{\Delta base} \sin \Psi_i) \qquad (3)$$

where

P_{Lio} = original active load at bus i,

Q_{Lio} = original reactive load at bus i,

K_{Li} = multiplier designating the load change at bus i as λ changes,

Ψ_i = power factor angle of load change at bus i,

$S_{\Delta base}$ = the chosen apparent power for scaling of λ .

Simulation of Active Power Generation

The active power generation can be simulated as
$$P_{Gi}(\lambda) = P_{Gio}(1 + \lambda K_{Gi}) \qquad (4)$$
where

P_{Gio} = active generation at bus i in the base case,

K_{Gi} = constant specifying the rate of change in generation as λ varies.

Base Case Solution

The base case solution of the above reformulated power flow equations $(\delta_0, V_0, \lambda_0)$ is known via a conventional power flow and the solution path is being sought over a range of λ . In general the dimension of the whole set of equations will be $2n_{pq} + n_{pv}$, where n_{pq} and n_{pv} are the number of PQ and PV buses respectively.

To solve the problem, the continuation algorithm starts from the base solution $(\delta_0, V_0, \lambda_0)$ and uses a predictor-corrector scheme to find the subsequent solutions $(\delta_1, V_1, \lambda_1)$, $(\delta_2, V_2, \lambda_2)$,.. until the target point is reached.

3.2 Predictor – Corrector Scheme

Differences between continuation techniques are usually due to how predictor and corrector steps are implemented. The predictor – corrector scheme in this paper is described as follows:

Predictor

The prediction is made by taking an appropriately sized step in a direction tangent to the solution path. The predictor process is to calculate the tangent vector and to make the prediction. The tangent vector can be obtained as

$$
\begin{bmatrix} F_\delta & F_V & F_\lambda \end{bmatrix} \begin{bmatrix} d\,\underline{\delta} \\ d\,\underline{V} \\ d\,\underline{\lambda} \end{bmatrix} = 0 \tag{5}
$$

On the left side of the equation is a matrix of partial derivatives multiplied by a vector of differentials. The former is the conventional power flow Jacobian augmented by a column (F_λ), while the later is the tangent vector being sought.

Once the tangent vector has been found by solving eqn. (5), the prediction can be made as follows:

$$
\begin{bmatrix} \underline{\delta}^* \\ \underline{V}^* \\ \lambda^* \end{bmatrix} = \begin{bmatrix} \underline{\delta} \\ \underline{V} \\ \lambda \end{bmatrix} + \sigma \begin{bmatrix} d\,\underline{\delta} \\ d\,\underline{v} \\ d\,\lambda \end{bmatrix} \tag{6}
$$

where "*" denotes the predicted solution for a subsequent value of λ (loading) and σ is a scalar that designates the step size.

Corrector

The predicted solution is then corrected by reformulating a new set of power flow equations. This new set of equations would be

$$
\begin{bmatrix} \underline{F}(\underline{x}) \\ X_k - \eta \end{bmatrix} = 0 \tag{7}
$$

where $\qquad \underline{X} = \begin{bmatrix} \underline{\delta} \\ \underline{V} \\ \lambda \end{bmatrix}, \qquad \underline{x} \in R^{2n_{pq} + n_{pv} + 1}$

Once a suitable index k and value of η are chosen, a slightly modified Newton - Raphson power flow method (altered only in that one additional equation and one additional state variable) can be used to solve the set of equations. This provides the correction required to modify the predicted solution found.

4. ALGORITHM SUMMARY

The proposed algorithm of estimating the energy based measure of proximity to voltage collapse by using transient energy function and continuation power flow is summarized as follows:
1. Run a conventional power flow to obtain the base case.
2. Run the continuation power flow, using equations (2- 7) to obtain the voltage profile for each load change scenario.
3. Determine for each load change, stable equilibrium point (δ° , V° , λ) and the unstable equilibrium point (δ^1 , V^1 , λ).
4. Determine the difference in energy at the above points using formula (1).
5. Obtain the energy curve, which is the energy over one parameter family of operating points.

5. SIMULATION RESULTS

The program used for obtaining these results is written with C – language. This program has two main parts. The first is the continuation power flow program [13]. The second part is the transient energy function and energy measure program, which is developed by [11].

System 1: **The New England Test System**

The proposed method to identify the energy measure is applied to the New England 10-machine 30-bus test system shown in Fig. 2. The system data is found in [10]. Since this system is popular for voltage stability research, various load increase scenarios have already been described in [1, 4, 5].

In this paper the first scenario from [1] is used as a verification case. In this case, the reactive load at bus 11 is increased, while keeping all other loads and generator MW outputs fixed until voltage collapse occurs. Fig. (3-a) depicts voltage profiles for bus 11, and the three buses near to bus 11. Fig. (3-b) depicts the system energy difference as the reactive load at bus 11 is

Fig. 2. Single line
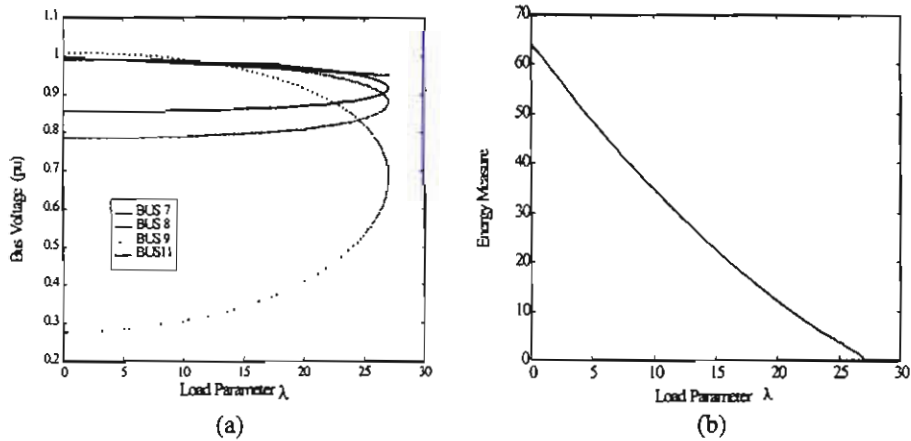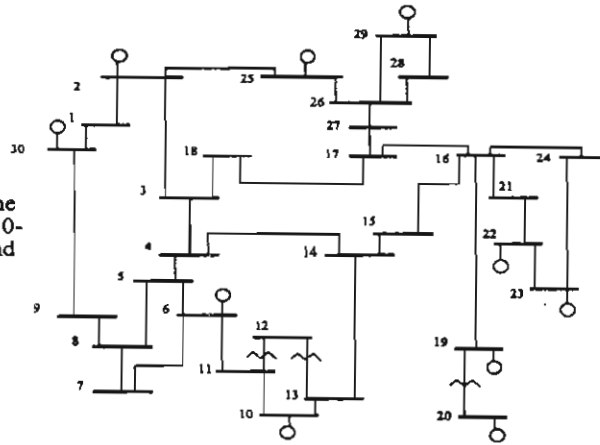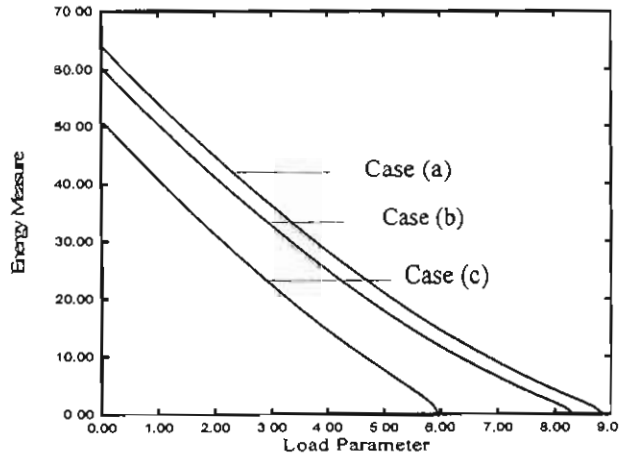diagram of the 30-
bus New England
test system.

Fig. 3. (a)Voltage profiles at buses [7,8,9,11], (b) System energy measure for reactive
power increasing at bus 11.

Fig. 4. System
energy measure
for active and
reactive power
increasing at
bus 3.

increased until voltage collapse occurs. Fig. (4) depicts the variation in the energy for the following cases:

(a) as λ is varied for the load at bus 3. The load is assumed to be a linear function of parameter λ as:

$$P = P_0 (1 + \lambda) \quad , Q = Q_0 (1 + \lambda) \tag{8}$$

(b) repeat the case (a) with generator no. 6 is removed, and

(c) repeat the case (a) in addition of the line (2-3) outage.

System 2: The Egyptian Unified Power Network

The data used in this section is a typical $500 - 220 - 132$ Kv modern Egyptian Unified Power Network (EUPN) for maximum loading at 1/4/1998 [12]. The single line diagram of the EUPN is shown in Fig. 5. This network is divided in 5 areas, with 24 generating stations, 107 - bus, 7 shunt reactors and 153 transmission lines and transformers, including 16 under-load tap changer (ULTC) transformers. The generation capacity is 10965.0 MW and the total load is 9104.3 MW and 5429.4 MVAR. Only two reactors (2×165 MVAR) are connected on bus no. 4 (High Dam) in the base case.

The system is studied without enforcing power flow control between areas, treating the ULTCs as regulator transformers with fixed taps, and considering the generator limits, which introduce extra nonlinearities into an already nonlinear system. Loads are assumed to be a linear function of a parameter λ ($\lambda = 0$ for base case). Four load increase cases are presented as follows:

Case 1

It involves increasing active power of all system buses by the same value. P_{LO} is simply multiplied. Similarly, P_{GO} is increased by the same value as the load, but the usual constant constraints are imposed on the reactive power output of the generators (Q_G). The voltage profile and energy measure are demonstrated for each of the following:

A. No contingency.

B. Outage of generator 53 and line (9-13).

Figure (6A) depicts the voltage profiles at the weakest buses (24, 8, 34, 25, 33, 35, 39 and the critical bus no. 36) and energy measure of the system
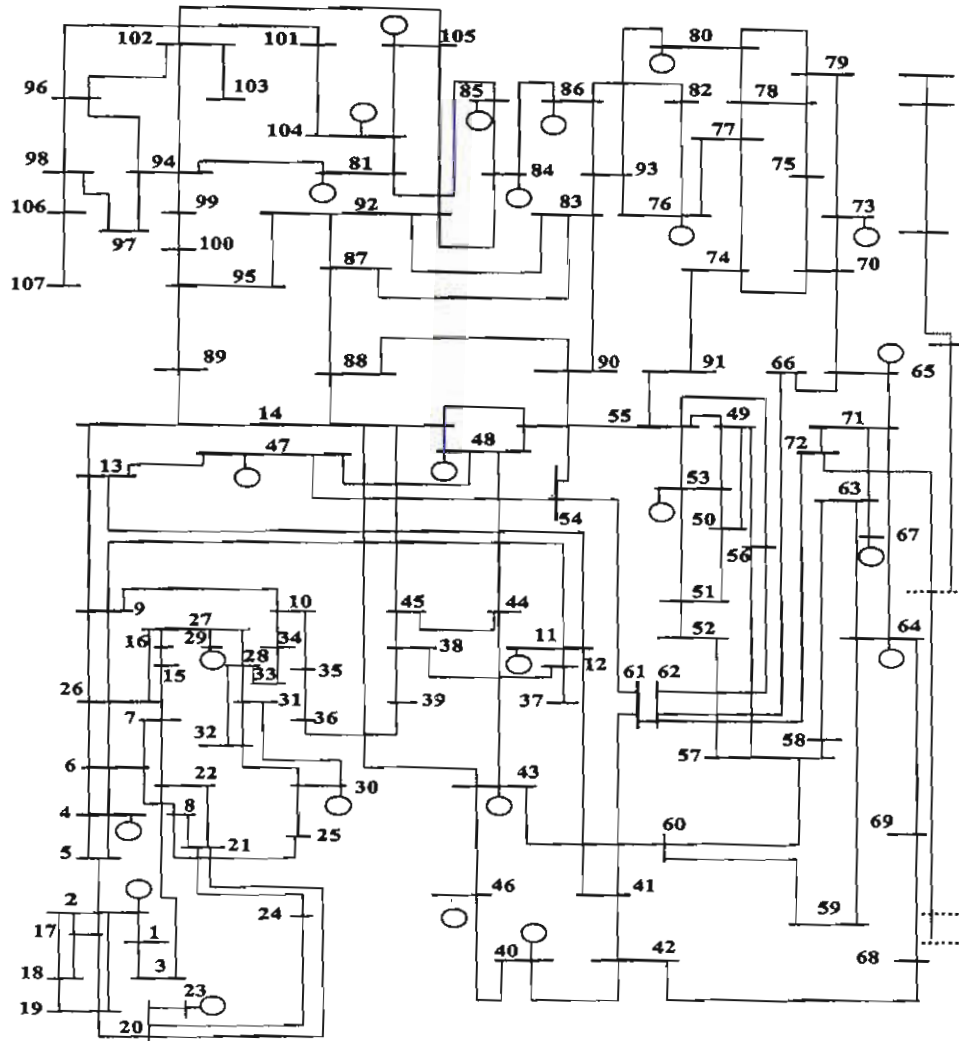
Fig. 5. Single line diagram of the 24 - Machine, 107 - bus (EUPN)

Table 1. Power Stations in the EUPN

Generator Bus No.	Name	Generator Bus No.	Name	Generator Bus No.	Name
2	ASWANDAM	46	WADI HOUF	76	TALKHA
4	HIGH DAM	47	C. WEST 500	80	DEMITTA
11	KURIMAT	48	C. WEST 220	81	KFR DAWAR
23	NEW ISNA	53	S.KHEMA	84	DAMAN GAS
29	WALIDIA	64	ATAKA	85	DAMAN GIS
30	ASSYUT	65	A. SOLTAN	86	MAHMODIA
40	NEW TEBBIN	67	SUEZ PS	104	ABIS
43	CAIRO SOUHT	73	PORT SAID	105	ABU KIR

without contingency. Twelve generators (at buses no. 23, 30, 40, 43, 48, 67, 73, 76, 81, 84, 85, and 104) are reached to their reactive limits.

Figure (6B) depicts the voltage profiles at the weakest buses (22, 8, 34, 25, 33, 35, 39 and the critical bus no. 36) and system energy measure in the case of removing generator at bus 53 and outage of line (9-13). Fifteen generators (at buses 11, 23, 30, 40, 43, 47, 48, 67, 73, 76, 81, 84, 85, and 104) are reached to their reactive limits.

Case 2

It involves increasing of active and reactive power of all system buses by the same value. P_{LO} and Q_{LO} are simply multiplied. Similarly, P_{GO} is increased by the same value as the load, but the usual constant constraints are imposed on the reactive power output of the generators (Q_G).

Figure (7A) depicts the voltage profiles at the weakest buses (24, 8, 25, 34, 33, 35, 36 and the critical bus no. 39) and energy measure of the system without contingencies. Fourteen generators (at buses 2, 23, 30, 40, 43, 47, 48, 53, 67, 73, 76, 81, 84, 85, and 104) are reached to their reactive limits.

Figure (7B) depicts voltage profiles at the weakest buses (10, 8, 25, 34, 33, 35, 36 and the critical bus no. 39) and system energy measure in the case of removing generator at bus 53 and outage of line (9-13). Sixteen generators (at buses 2,11, 23, 29, 30, 40, 43, 47, 48, 67, 73, 76, 81, 84, 85, and 104) are reached to their reactive limits.

Case 3

It involves increasing P_L, Q_L and P_G, as in case 2, on buses of Upper Egypt area (buses 1 - 39). Figure (8) depicts the variation in the energy measure for the cases: (a) without contingencies, (b) repeat case (a) with generator no. 29 is removed, (c) repeat case (a) with outage of line (9-11), and (d) repeat case (a) with generator no. 29 is removed in addition of the line (9-11) outage.

Case 4

It involves increasing P_L, Q_L and P_G, as in case 2, on buses of Cairo area (buses 40 - 62). Figure (9) depicts the variation in the energy measure for the cases: (a) without contingecy, (b) repeat case (a) with generator no. 53 is removed, (c) repeat case (a) with outage of line (54-61), and (d) repeat case
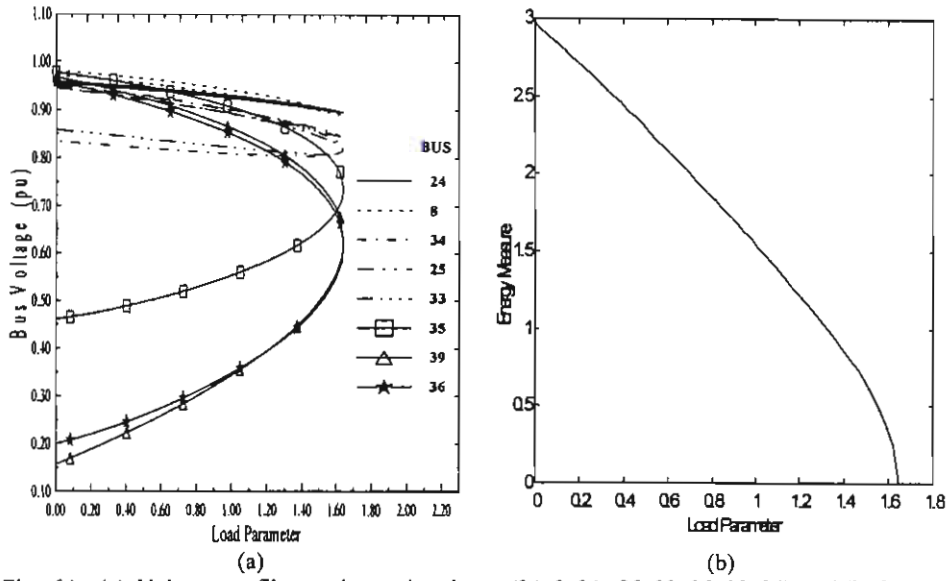
Fig. 6A: (a) Voltage profiles at the weakest buses (24, 8, 34, 25, 33, 35, 39, 36), and (b) System energy measure. For active power increasing at all system buses without contingency
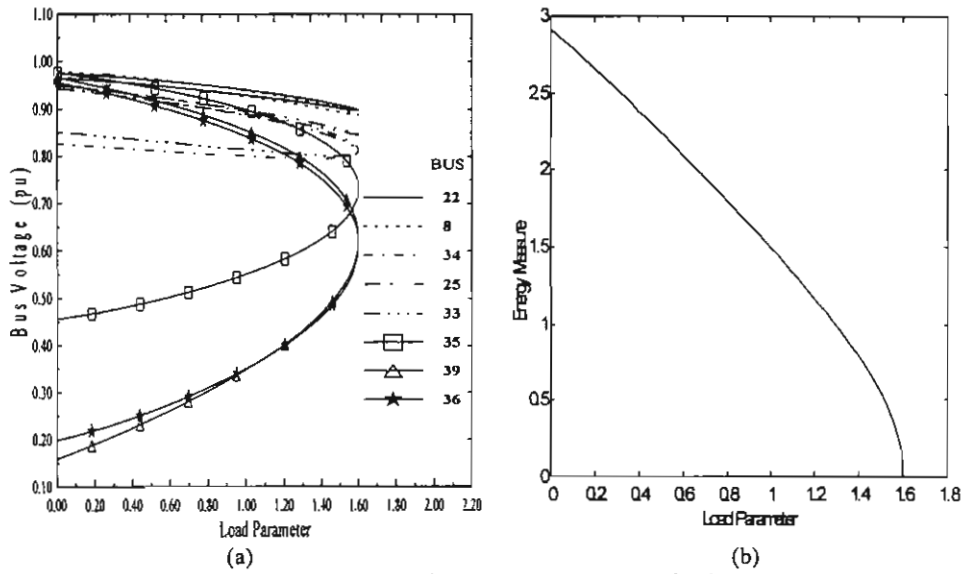

Fig. 6B. (a) Voltage profiles at the weakest buses (22, 8, 34, 25, 33, 35, 39, 36), and (b) System energy measure. For active power increasing at all system buses with removing generator at bus 53 and outage of line (9-13).

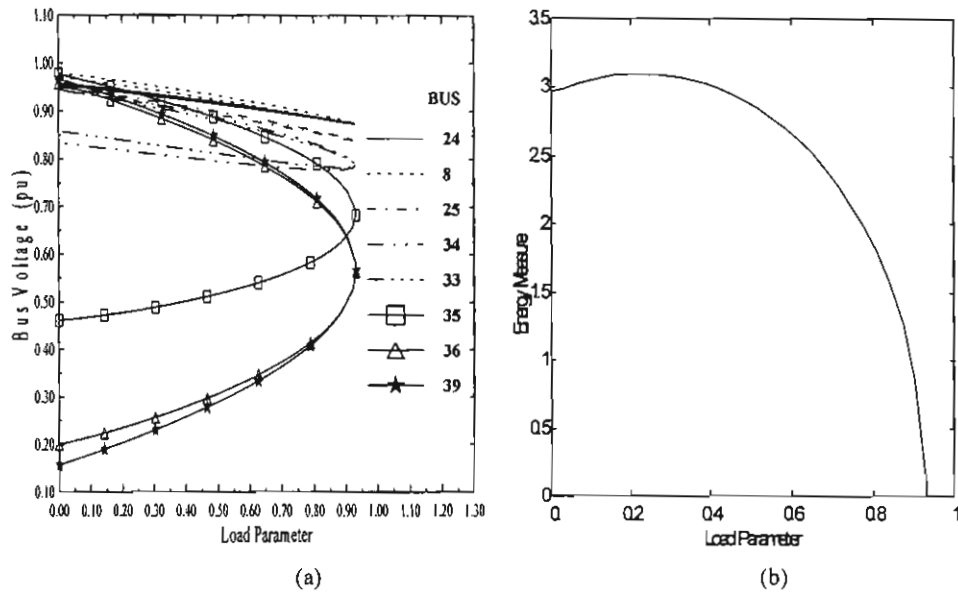(a)   (b)

Fig. 7A: (a) Voltage profiles at the weakest buses (24, 8, 25, 34, 33, 35, 36, 39), and (b) System energy measure. For active and reactive power increasing at all system buses.

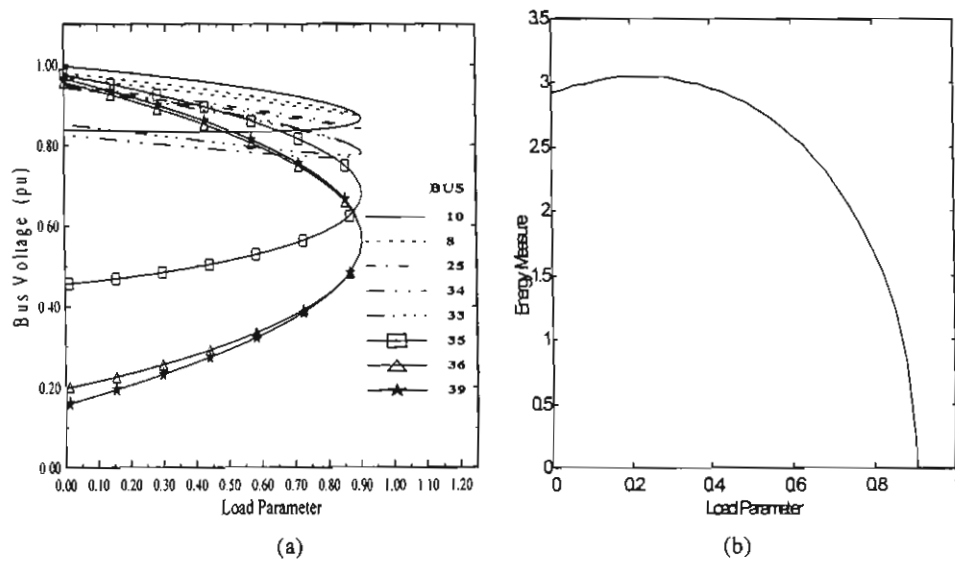(a)   (b)

Fig. 7B. (a) Voltage profiles at the weakest buses (10, 8, 25, 34, 33, 35, 36, 39), and (b) System energy measure. For active and reactive power increasing at all system buses with removing generator at bus 53 and outage of line (9-13).
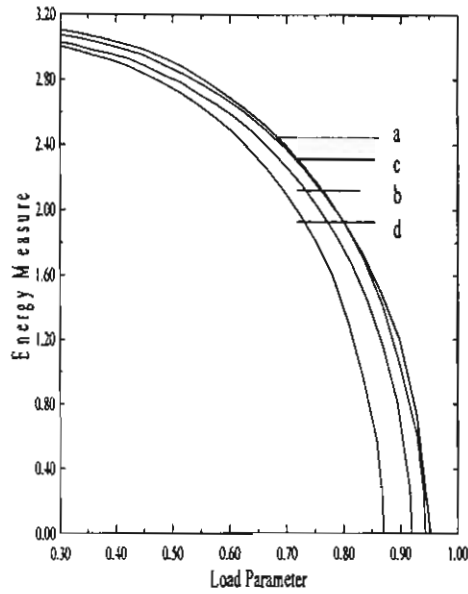
Fig. 8. System energy measure for different contingencies in Upper Egypt area (buses 1 - 39)
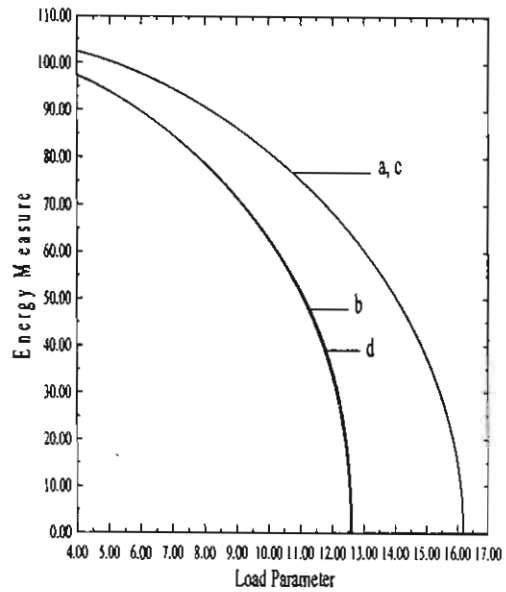
Fig. 9. System energy measure for different contingencies in Cairo area (buses 40 - 62)

(a) with generator no. 53 is removed in addition of the line (54-61) outage.

Table 2 illustrates the generator buses reached to reactive power limits and the corresponding critical bus in cases No. 3 and 4.

Table 2.

Case	Area		Critical Bus	
	Upper Egypt	Cairo	Upper Egypt	Cairo
a	2, 30, 40, 43, 47, 48, 73, 85, 104.	23, 30, 40, 43, 47, 48, 73, 85, 104.	39	44
b	23, 30, 40, 43, 47, 73, 85, 104.	23, 30, 40, 43, 47, 48, 73, 85, 104.	39	44
c	2, 23, 29, 30, 40, 43, 48, 73, 85, 104.	30, 40, 43, 48, 73, 85, 104.	36	44
d	23, 30, 40, 43, 47, 48 , 73, 85, 104	23, 30, 40, 43, 48, 73, 85, 104.	39	44

6. CONCLUSION

Voltage stability assesment by using the transient energy function and continuation power flow is presented. The transient energy function provids a measure of the energy difference between two equilibrium points. The problem of identifying the second equilibrium point (unstable equilibrium point), required in the procedure, is overcomed by the continuation power flow. The results presented in the paper demonstrate that the energy measures are quite smooth and there is no discontinuities, especially when generator maximum active power and reactive power limits are reached and switched from PV to PQ. The proposed method is capable and useful to find the critical bus and to assess voltage stability by using energy measure for different scenarios of the Egyptian Unified Power Network.

7. REFERENCES

[1] Y. Tamura, H. Mori and S. Iwamoto, " Relationship Between Voltage Instability and Multiple Load Flow Solutions in Electric Power Systems", IEEE Trans. Power App. and Sys., Vol. PAS-102, No. 5, pp. 1115-1125, May 1983.

[2] M.M. EL-Kateb, S. Abdelkader, M.S. Kandil, "Linear Indicator for Voltage Collapse in Power Systems ", IEE Proc. Gener., Transm. Distrib., Vol. 4, No. 2, March 1997.

[3] C. Rajagopalan, B. Lesieutre, P. W. Sauer, M. A. Pai, "Dynamic Aspects of Voltage/Power Characterestics", IEEE Trans. on Power Sys., Vol. 7, No. 3, pp. 990-1000, Aug. 1992.

[4] C.L. Demarco and T.J. Overbye, "An Energy Based Security Measure for Assessing Vulnerability to Voltage Collapse", IEEE Trans. on Power Sys., Vol. 5, No.2, pp 419-427, May 1990.

[5] V. Ajjarapu and C. Christy, "The Continuation Power Flow: A Tool for Steady State Voltage Stability Analysis", IEEE Trans. on Power Sys. ,Vol. 7, No. 1, Feb. 1992.

[6] A. A. Fouad, S. E. Stanton, "Transient Stability of a Multi-Machine Power System. Part 1: Investigation of System Trajectories", IEEE Trans. on Power App. and Sys. ,Vol. PAS-100, No. 7, pp 3408-3416, July 1981.

[7] Farrokh A. Rahimi, Mark G. Lauby, Joseph N. Wrubel, Kwok L. Lee, "Evaluation of the Transient Energy Function Method for On-Line Dynamic Security Analysis", IEEE Trans. on Power Sys. ,Vol. 8, No. 2, pp 497-507, May 1993.

[8] C. L. Demarco and Claudio A. Canizares, "A Vector Energy Function Approach for Security Analysis of AC/DC Systems", IEEE Trans. On Power Sys., Vol. 7, No. 3, pp 1001-1011 Aug. 1992.

[9] M. A. Pai , Energy Function Analysis for Power System Stability , Kluwer Academic, 1992.

[10] R. A. Schluter, A.G. Costi,   J. E. Sekerke and H.L. Forgy, "Voltage Stability and Security Assessment", EPRI Report, El-5967, Project 1999-8, Aug. 1988.

[11] A. A. Attia and H. A. Abdelsalam, "An Efficient Algorithm to Assess Voltage Stability Based on Transient Energy Function", Six Middle-East Power Systems Conference (MEPCON'98), Mansoura, Egypt, pp 740-745, Dec. 1998.

[12] Minstray of Electricity and Egyptian Authority (1998): The Unified Electrical Network, A.R.E., 30 – 500 KV directory.

[13] H.-D. Chiang, A. J. Flueck, K. S. Shah, and N. Balu,"CPFLOW: A Practical tool for Tracing Power System   Steady State Stationary Behavior Due to Load and Generation Variations," IEEE Trans. on Power Sys. ,Vol. 10, No. 2, May 1995.